Jpn. J. Appl. Phys. Vol. 37 (1998) pp. 135–140
Part 1, No 1, January 1998

Pressure Induced Phase Transitions in Spinel and Wurtzite Phases of $ZnAl_2S_4$ Compound

Veacheslav V. URSAKI[1], Igor I. BURLAKOV[1], Ivan M. TIGINYANU[1], Yannis S. RAPTIS[2], Evangelos ANASTASSAKIS[2], Igor AKSENOV[3] and Katsuaki SATO[4,*]

[1] *Institute of Applied Physics, Academy of Sciences of Moldova, Kishinev 2028, Moldova*
[2] *Physics Department, National Technical University, 15780 Athens, Greece*
[3] *Joint Research Center for Atom Technology, 1-1-4 Higashi, Tsukuba, Ibaraki 305, Japan*
[4] *Faculty of Technology, Tokyo University of Agriculture and Technology, Koganei, Tokyo 184, Japan*

(Received July 14, 1997; accepted for publication October 20, 1997)

$ZnAl_2S_4$ single crystals with spinel (α-phase) and wurtzite (w-phase) structures have been studied by Raman spectroscopy under hydrostatic pressures of up to 300 kbar. Significant changes in the phonon spectrum of the α-phase have been observed at the critical pressure of 230 kbar, which are attributed to a reversible phase transition to a denser high-pressure phase, having a similar structure to that of calcium ferrite. In the pressure interval of 180 to 230 kbar, the two phases coexist. The irreversible disappearance of the Raman signal of w-$ZnAl_2S_4$ doped by Cd at pressures above 90 kbar was attributed to a phase transition to a rocksalt-type structure. This critical pressure is 40 kbar lower than that in undoped w-$ZnAl_2S_4$ and is explained on the basis of crystal structure quality. Different structures were realized upon removing the pressure, depending on the highest pressure previously reached, such as a mixture of wurtzite and spinel phases, a spinel quasi-crystalline structure, or a pressure-induced amorphous phase. The behavior of the quasi-crystalline spinel structure upon repeating the pressure cycle was found to be different from that of the α-phase single crystal.

KEYWORDS: $ZnAl_2S_4$, spinel, wurtzite, high-pressure, Raman spectroscopy, phase transitions, pressure-induced amorphization

1. Introduction

Structural studies of semiconductors have become a fundamental problem of high-pressure science since the discovery of pressure-induced phase transitions. A systematic structural study of the standard II–VI, III–V and group IV semiconductors has been undertaken over the past few years.[1–3] While considerable efforts were put on the study of pressure-induced phase transitions in I–III–VI_2 chalcopyrites,[4–6] only a single high-pressure study has been reported on II–III_2–VI_4 ordered vacancy compounds.[7] Since these materials crystallize in different structures, depending on the growth conditions,[8–10] their behavior under hydrostatic pressure appears to be an interesting problem. One of the most important materials in this regard is $ZnAl_2S_4$ which can be obtained as different structural modifications, depending on growth temperature.[11,12] Three phases exist in the region of low-growth temperatures (700–900°C), namely, the spinel structure (α-phase), the wurtzite-type structure with a statistical distribution of the cations, called w-phase, and the layered structure with a hexagonal lattice, called the L- or γ/-phase. At high-growth temperatures (1050–1100°C) an orthorhombic β-phase and a rhombohedral γ-phase can be obtained. Furthermore, quaternary solid solutions $ZnAl_{2(1-x)}Ga_{2x}S_4$ (obtained by adding gallium atoms to the Zn–Al–S system) crystallize in a defect chalcopyrite (DC) structure.[13] In this work, we present the results of a structural study of α- and w-type phases of $ZnAl_2S_4$ under hydrostatic pressure of up to 300 kbar.

2. Experimental

The α- and w-phase $ZnAl_2S_4$ crystals were grown by the chemical transport technique, with iodine used as the transport agent. The initial elements Zn, Al and S (total mass 2–2.5 g) were loaded in quartz ampoules (15 mm in diameter, 15 cm in length). For the α-phase, the temperatures at the charge and growth zones were 850 and 750°C, respectively. The spinel structure of the single crystals was confirmed through X-ray analysis, with a lattice parameter of 10.01 Å; w-phase crystals were obtained when the growth temperature was 50°C lower than that for the α-phase. Two types of w-$ZnAl_2S_4$ crystals were grown, one with full stoichiometry and a second one with about 10 % of the Zn atoms substituted by Cd atoms. According to the X-ray analysis, both types of w-$ZnAl_2S_4$ crystals possess a random distribution of cations and stoichiometric vacancies among the possible tetrahedral sites of the lattice, with unit cell parameters of $a = 3.76$ Å and $c = 6.15$ Å.[14]

Unpolarized Raman spectra were taken in a diamond anvil cell at ambient temperature. The pressure was calibrated to within 0.1 kbar using the ruby luminescence lines. The Raman spectra were measured with a double spectrometer in nearly back-scattering geometry. The 514.5 nm line of an argon laser was used at power levels of approximately 30 mW. The laser spot on the sample was 50 μm and the resolution was better than 1 cm^{-1}.

3. Results and Discussion

3.1 α-phase of $ZnAl_2S_4$

The α-$ZnAl_2S_4$ exhibits a normal spinel structure (space group Fd3m) with two formula units per unit cell. The ideal spinel structure consists of a cubic closed array of anions in which one-third of the cations (Zn) are on tetrahedrally coordinated sites and two-thirds of the anions (Al) are on octahedrally coordinated sites. The presence of vacancies in the crystal structure results in distortions in the anion sublattice. This effect is usually quantified by the so-called internal distortion parameter u, the value of which is 3/8 for the ideal fcc structure. In the case of α-$ZnAl_2S_4$ it is equal to 0.385.

Forty-two normal vibrations are expected in a normal spinel structure at $k = 0$.[15] These vibrations are described by the following reduction into the irreducible representations of the point group,

*To whom reprint requests should be addressed
E-mail: satokats@cc.tuat.ac.jp

$$\Gamma = A_{1g} + E_g + T_{1g} + 3T_{2g} + 2A_{2u} + 2E_{2u} + 5T_{1u} + 2T_{2u}. \quad (1)$$

One of these modes (T_{1u}) is acoustic, four (T_{1u}) are IR active and five (A_{1g}, E_g, $3T_{2g}$) are Raman active. The remaining modes (T_{1g}, A_{2u}, E_{2u}, T_{2u}) are inactive.

Figure 1 shows unpolarized Raman spectra of α-$ZnAl_2S_4$ at various pressures. Only three Raman-active modes (E_g, A_{1g} and T_{2g}) are observed under ambient conditions at 133, 353 and 413 cm^{-1}, respectively. The assignments of these modes are based on previously published polarization data at zero pressure.[16]

Figure 2 illustrates the Raman shifts as a function of pressure. A monotonous shift to higher frequencies is a characteristic of all the modes observed. The linear and quadratic pressure coefficients of Raman shifts obtained from a least squares fit are listed in Table I along with their relative slopes $(1/\omega_0)(d\omega/dP)$ which are related to the mode Grüneisen parameters γ through

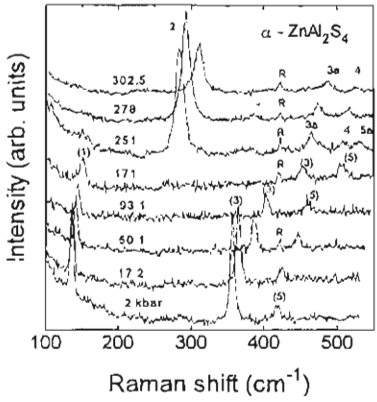

Fig. 1. Unpolarized Raman spectra of α-$ZnAl_2S_4$ at various pressures and room temperature. R corresponds to a sapphire Raman line.

Table I. Pressure dependence of Raman-active phonon frequencies of α-$ZnAl_2S_4$. The parameter ω_0 is in units of cm^{-1}, a is in units of $10^{-1}\cdot cm^{-1}\cdot kbar^{-1}$, b in units of $10^{-4}\cdot cm^{-1}\cdot kbar^{-2}$, and $(1/\omega_0)(d\omega/dP)$ in units of $10^{-4}\cdot kbar^{-1}$

Band Number	ω_0	a	b	$(1/\omega_0)(d\omega/dP)$
1	133	1.05	−1.35	7.9
2	185	3.93	—	21.2
3	353	5.45	−1.80	15.4
3a	414	2.26	—	5.6
4	446	2.54	—	5.7
5	413	4.99	−1.02	12.1
5a	446	2.61	—	5.6

$$\gamma = (1/\beta)(1/\omega_0)(d\omega/dP). \quad (2)$$

where β is the isothermal volume compressibility, not available at present. The intensity of all modes was found to decrease with pressure (Fig. 3, inset). A significant transformation of the Raman spectrum may be noticed at the critical pressure $P_c = 230$ kbar. The disappearance of the E_g band (#1, Figs. 1, 2, 3) and the emergence of two new bands (#2, #4, Figs. 1, 2), is very dramatic. The behavior of the mode intensities normalized to the intensity of the A_{1g} (3) peak is shown in Fig. 3. The decrease in the intensity of the spinel mode is accompanied by an enhancement of modes #2 and #4, the former being the dominant one. With decreasing pressure, all the new modes exhibit a hysteresis and they disappear completely at 180 kbar. As the pressure is completely released, the initial Raman spectrum is fully recovered.

Next we discuss the changes in the Raman spectrum observed at 230 kbar; the value of this critical pressure was determined from the extrapolation to zero of the A_{1g} mode intensity (Fig. 3, inset). We note here that $MgAl_2O_4$ which crystallizes with a perfect spinel structure, undergoes, at pressures above 250 kbar, a phase transition to a high-pressure phase with a similar structure to that of calcium ferrite (see X-ray powder diffraction data in ref. 17. The calcium ferrite structure belongs to the D_{2h}^{16} (Pnam) space group and is the most dense structure among all known crystalline materials

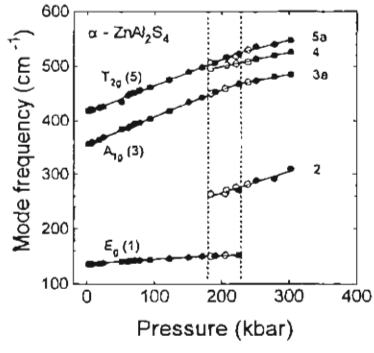

Fig. 2. Pressure dependence of the Raman-active modes observed in Fig. 1. Full and open circles correspond to the increase and decrease of the pressure, respectively. Solid lines are the quadratic (linear) least squares fits for the low (high) pressure phase. The numbers in parentheses correspond to spinel structure; those without parentheses to calcium ferrite structure. Both types of structures are presented in Table I.

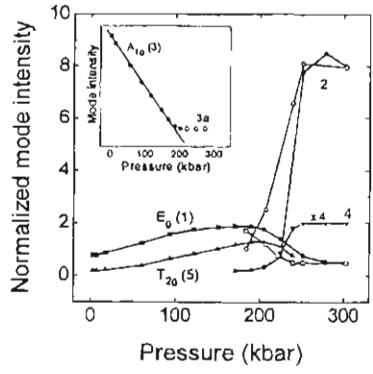

Fig. 3. Scattering intensity (normalized to that of the A_{1g} mode) for some of the modes of Table I, as a function of pressure. The inset shows how the pressure of 230 kbar is determined. Solid lines and full circles correspond to increasing pressure; dashed lines and open circles correspond to decreasing pressure.

with the AB_2O_4 composition, in which A^{2+} ions are located in eight-coordinated sites and the B^{3+} ions in octahedral sites. Its unit cell consists of four formula units. According to group theory, one should expect four types of Raman active modes (A_g, B_{1g}, B_{2g}, B_{3g}) and three types of IR active modes (B_{1u}, B_{2u}, B_{3u}). On the basis of the correlation between the Raman active modes of the two point groups (O_h and D_{2h}), one finds that the A_{1g} and E_g modes in the O_h representation transform to the A_g and $2A_g$ modes, respectively, in the D_{2d} representation, and the T_{2g} modes transform to the $B_{1g}+B_{2g}+B_{3g}$ modes. The parallel behavior of the new mode #2 and the spinel E_g (1) mode in the pressure increase and decrease allows us to assume that the mode #2 is of A_g symmetry. Two additional new modes, namely #4 and #5a, exhibit similar behavior; they correlate to the T_{2g} (5) spinel mode and as such they should have $B_{(1,2,3)g}$ symmetry. As for #3a mode, its symmetry is A_g since it originates from the A_{1g} (3) spinel mode.

3.2 *w-phase of $ZnAl_2S_4$*

There are no calculations of the phonon spectrum of w-$ZnAl_2S_4$. The crystal structure of w-$ZnAl_2S_4$ is similar to that of w-ZnS. According to the X-ray analysis, both materials belong to the space group C_{6v}[4,14] and have nearly the same unit cell parameters ($a = 3.811$ Å and $c = 6.234$ Å for w-ZnS).[18] At the same time, the phonon spectrum of w-$ZnAl_2S_4$ proves to be more complicated than that of w-ZnS.

Figures 4 and 5 show the Stokes Raman spectra of undoped and Cd-doped w-$ZnAl_2S_4$ crystals, respectively for various pressures up to approximately 120 kbar. Unlike in undoped crystals, the defect-induced second-order broad Raman bands are absent in Cd-doped crystals. This indicates that the addition of Cd atoms in w-$ZnAl_2S_4$ leads to a considerable improvement in the crystal quality.

In order to analyze the pressure dependence of the various modes in Figs. 4 and 5, a multiple-band fitting of the spectra was used. The mode frequencies were found to increase with increasing pressure. The shifts as a function of pressure are shown in Fig. 6. The linear and quadratic pressure coefficients of the Raman shifts are the same for both Cd-doped and undoped crystals and listed in Table II together with their relative slopes $(1/\omega_0)(d\omega/dP)$.

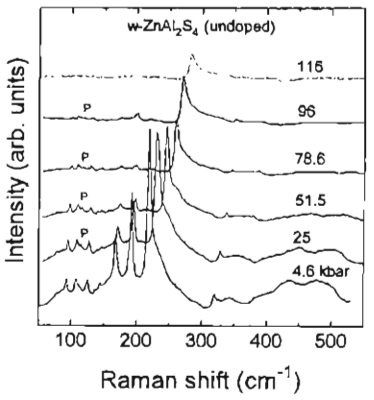

Fig. 4. Raman spectra of undoped w-$ZnAl_2S_4$ at various pressures and room temperature. P is a laser plasma line.

It is apparent that some of these modes (namely W4, W7 and W9–W21) are very similar to the modes inherent in the defect-chalcopyrite phase of $ZnAl_2S_4$,[13] where the stoichiometric vacancies and cations are strictly ordered. In w-$ZnAl_2S_4$ the cations and vacancies are randomly distributed. However, at the microscopic level, each randomly distributed cation and stoichiometric vacancy occupies certain tetrahedral sites. Consequently, one can assume that the above mentioned modes have a local-type character. Apart from that, the pressure behavior of the most intense of these modes (W10) is analogous to the so-called "breathing" mode which is caused by symmetric oscillations of anions surrounding the stoichiometric vacancy in defect-chalcopyrite $CdAl_2S_4$.[7]

As the pressure increases up to 60–70 kbar, the intensity of the local-type modes in Cd-doped w-$ZnAl_2S_4$ increases. Beyond this pressure, the intensities start to decrease sharply (see, for instance, mode W10 in Fig. 7). At the same time,

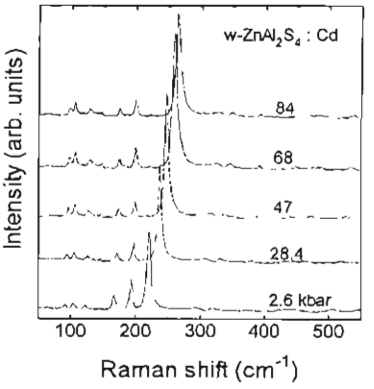

Fig. 5. Stokes Raman spectra of Cd-doped w-$ZnAl_2S_4$ at various pressures and room temperature.

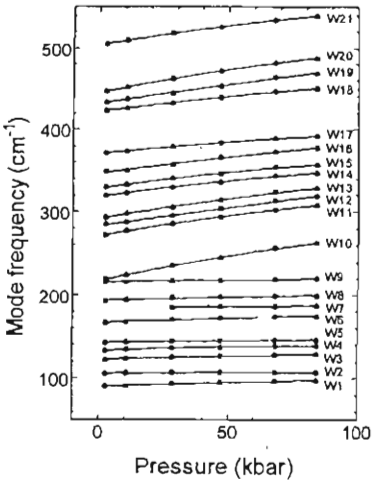

Fig. 6. Pressure dependence of Raman-active modes of w-$ZnAl_2S_4$. Solid lines are quadratic least squares fits. The mode notation on the right-hand side corresponds to that of Table II.

Table II. Pressure dependence of Raman-active phonon frequencies of w-type $ZnAl_2S_4$. The units are as in Table I.

Mode	ω_0	a	b	$(1/\omega_0)(d\omega/dP)$
W1	91	0.85	—	9.4
W2	106	0.16	—	1.5
W3	123	0.80	—	6.5
W4	133	1.50	−9.69	11.3
W5	143	0.43	—	3.0
W6	167	0.99	—	5.9
W7	184	0.61	−2.51	3.3
W8	194	0.74	—	3.8
W9	216	0.49	—	2.3
W10	217	6.88	−17.50	31.7
W11	271	5.67	−15.04	20.9
W12	283	4.49	−2.43	15.9
W13	292	5.50	−13.04	18.8
W14	318	4.45	−11.60	14.0
W15	328	4.68	−14.33	14.3
W16	347	4.37	−8.20	12.6
W17	371	3.34	−9.61	9.0
W18	422	4.10	−8.45	9.7
W19	432	4.64	−2.39	10.7
W20	444	6.82	−19.86	15.4
W21	504	5.33	−14.17	10.6

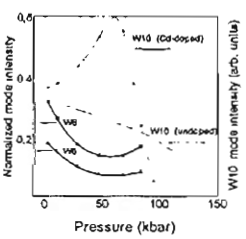

Fig. 7. Pressure dependence of the intensity of the W10 mode ($217\,cm^{-1}$ at $P = 0$, intensity axis on the right-hand side) for Cd-doped and undoped crystals, and normalized intensities for the Cd-doped W6 and W8 modes relative to that of the Cd-doped W10 mode.

the remaining modes (W1–W3, W5, W6 and W8) decrease in intensity, when normalized to the W10 mode, up to the pressure of approximately 60 kbar. In our opinion, this behavior is an indication that some ordering of cations takes place at approximately 60 kbar. It is to be noted that in the case of the complete ordering of cations we obtain the β-phase, which can be regarded as having a wurtzite-derivative structure; in the latter, the anions are arranged in hexagonal close packing, whereas Zn and Al atoms and vacancies are distributed in an ordered manner over tetrahedral sites.

The decrease of mode intensities beyond 60 kbar in Cd-doped crystals is attributed to lattice deformations prior to the high-pressure phase transition, as confirmed by the pressure dependence of full-width at half maximum (FWHM) of the Raman modes (see W10 mode in Fig. 8). As the pressure increases up to 60 kbar, the W10 mode exhibits a slight decrease of FWHM, whereas the FWHM increases for $P > 60$ kbar.

At about 90 kbar the Raman signal disappears completely and irreversibly in Cd-doped w-$ZnAl_2S_4$ (see Fig. 7 for the W10 mode). This change with increasing pressure is attributed to a phase transition to a high-pressure structure with sixfold coordination, most likely of rocksalt type. Moreover, some changes in the crystal structure are already initiated at 60 kbar.

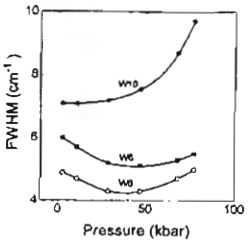

Fig. 8. FWHM for the Cd-doped W10, W6 and W8 modes as a function of pressure.

It should be noted that the critical pressure for the phase transition to the Raman-inactive phase is different for undoped and Cd-doped w-$ZnAl_2S_4$ crystals (130 kbar and 90 kbar, respectively, see W10 mode in Fig. 7). We conclude that the more defective the material, the higher the pressure of phase transition. The Raman signal in both cases is recovered only below 10 kbar and the shape of the spectrum is different.

The Raman spectrum of undoped w-$ZnAl_2S_4$ which was recovered below 10 kbar, was not the same as the initial one and exhibited distinct signs of amorphization. Such a pressure-induced amorphization process has been previously observed in tetrahedrally bonded materials.[19,20] It has been established that amorphization occurs if pressure is released in certain temperature intervals. Above this interval, the initial crystal structure is recovered. A pressure release below this interval leads to a quenching of the high-pressure phase. In this case, amorphization from the quenched high-pressure phase occurs when the temperature is elevated at a low pressure. In our case of w-$ZnAl_2S_4$, the room temperature is within the critical temperature interval for amorphization. Thus, an amorphous phase of w-$ZnAl_2S_4$ is obtained when pressure is released at room temperature. The degree of amorphization depends on how far from the point of phase transition to the Raman-inactive phase is the pressure increased (see Fig. 9). If the maximum pressure reached is P_{max} = 130 kbar, the features of the initial crystalline structure are fully recovered upon releasing pressure. If $P_{max} \geq 150$ kbar, full amorphization is observed. An analogous behavior was observed in ZB III–V compounds.[21,22] It was shown that the amount of amorphous phase produced increases with P_{max}, by analogy to the increase observed as the dose increases in heavy ion-implanted GaAs.[21] Furthermore, the long-range order observed in GaP samples after pressure release has been shown to depend on P_{max}.[22]

Figure 10 illustrates the Raman spectra of Cd-doped w-$ZnAl_2S_4$ after pressure release, for two different values of P_{max}. For $P_{max} = 100$ kbar we have a mixture of two phases. The Raman spectrum also exhibits a new peak (S, for spinel) besides the ones characterizing the w-phase. The position of this new peak is very close to the E_g mode in α-$ZnAl_2S_4$ (see Figs. 1, 2). We conclude that we have a mixture of α- and w-phases. For $P_{max} = 110$ kbar, the peaks characteristic of the w-phase disappear after pressure release, the remaining peak

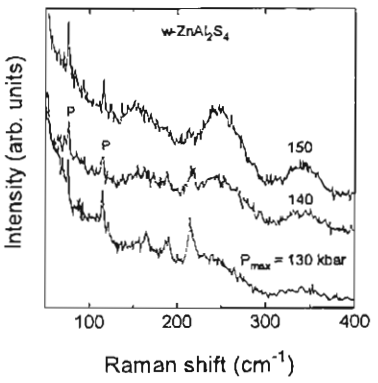

Fig. 9. Raman spectra of undoped w-$ZnAl_2S_4$ after pressure release, for P_{max} = 130, 140, 150 kbar. P are laser plasma lines.

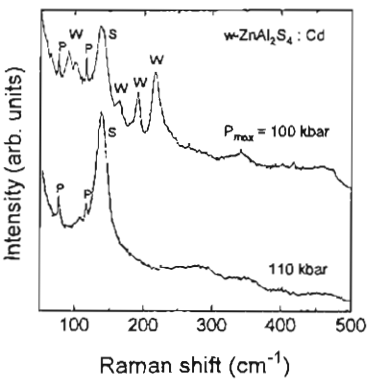

Fig. 10. Raman spectra of Cd-doped w-$ZnAl_2S_4$ after pressure release for P_{max} = 100 and 110 kbar.

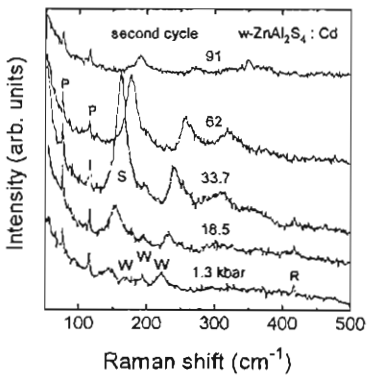

Fig. 11. Raman spectra of Cd-doped w-$ZnAl_2S_4$ after pressure release, during the second pressure cycle. R is a sapphire Raman line and P are laser plasma lines.

presumably originating from the α-phase.

Figure 11 shows the Raman spectra of w-$ZnAl_2S_4$:Cd at various pressures, after the initial release. As shown in

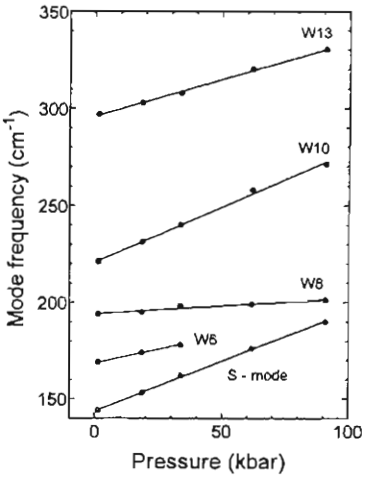

Fig. 12. Pressure dependence for some of the modes discussed, and for the new S mode during the second pressure cycle, in Cd-doped w-$ZnAl_2S_4$. The solid lines are linear least squares fits. The mode notation corresponds to Table III

Table III. Pressure dependence of Raman-active phonon frequencies of Cd-doped w-$ZnAl_2S_4$ during a second pressure cycle. The units are as in Table I.

Mode	ω_0	a	$(1/\omega_0)(d\omega/dP)$
S-type	144	5.13	35.63
W6	169	2.78	16.45
W8	196	0.78	4.02
W10	221	5.67	25.65
W16	296	3.73	12.60

Fig. 12, there is a monotonous shift to higher frequencies for four wurtzite modes and one S mode (S). The linear pressure coefficients of these Raman shifts, obtained from a least-squares fit, are listed in Table III along with their relative slopes $(1/\omega_0)(d\omega/dP)$.

There are some differences in the behavior of the S (Fig. 12) and E_g (1) modes (Fig. 2), owing to the very defective type of the α-phase obtained after pressure release (probably its structure is most likely quasi-crystalline). Furthermore, the pressure dependence of the S-mode intensity and FWHM (Fig. 13) differs from that of the E_g (1) mode. The parameters for the first and second pressure cycle for w-modes are also different. Namely, the local-type modes become less sensitive to the pressure [smaller $(1/\omega_0)(d\omega/dP)$], while the other modes become more sensitive to the pressure [larger $(1/\omega_0)(d\omega/dP)$]. The increase of the S-mode intensity and decrease of FWHM for $P \leq 40$ kbar suggests that a recrystallization process of the destroyed α-phase takes place at intermediate pressures. The behavior of the S-mode for $P \geq 50$ kbar differs from that of the E_g (1) mode in the single crystal α-phase. The latter is stable for $P \leq 230$ kbar where a phase transition to the new phase occurs, as mentioned above, while the S-mode disappears near 100 kbar, indicating a phase transition to a Raman-inactive phase. In order to clarify the nature of this phase transition, an X-ray analysis under pres-

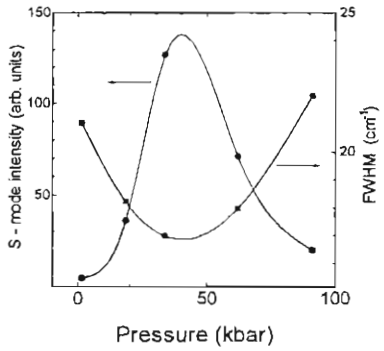

Fig 13. Pressure dependence of the S-mode intensity and FWHM.

sure is required. It is noted that a similar difference in the properties of crystalline and decompressed material has been observed in GaN[23] and explained by invoking nanocrystal structures.

Finally, for $P \geq 130$ kbar, the behavior of the Cd-doped w-$ZnAl_2S_4$ is similar to that of the undoped w-$ZnAl_2S_4$, in the sense that amorphization sets in after pressure release.

4. Conclusions

Spinel-type $ZnAl_2S_4$ single crystals transform to a denser structure, similar to that of calcium ferrite, at $P \approx 230$ kbar. In the interval between 180 and 230 kbar, the two phases coexist under increasing and decreasing pressure, according to the Raman data. Cd-doped $ZnAl_2S_4$ single crystals of wurtzite structure undergo a phase transition to a Raman-inactive rocksalt-type structure at $P \approx 90$ kbar, which is 40 kbar lower than that of undoped w-$ZnAl_2S_4$. Partial ordering of cations is confirmed below this transition, at 60 kbar.

After pressure release, any of the following structures may occur, depending on the maximum pressure reached: (i) a mixture of spinel and wurtzite phases, (ii) a quasi-crystalline spinel structure, and (iii) a pressure-induced amorphous phase. The behavior of the quasi-crystalline spinel structure during a second pressure cycle is different from that of the single-crystal α-phase. The α-phase of $ZnAl_2S_4$, therefore, appears to be a harder and more stable structure at elevated pressures.

1) M. I. McMahon and R. J. Nelmes: J. Phys. Chem. Solids **56** (1995) 485.
2) R. J. Nelmes, M. I. McMahon, N. G. Wright, D. R. Allan, H. Liu and J. S. Loveday: J. Phys. Chem. Solids **56** (1995) 539.
3) R. J. Nelmes, M. I. McMahon, N. G. Wright and D. R. Allan: J. Phys. Chem. Solids **56** (1995) 545.
4) J. Gonzalez, B.J. Fernandez, J. M. Besson, M. Cauthier and A. Polian: Phys. Rev. B **46** (1992) 15092.
5) T. Tinoko, A. Polian, J. P. Itie, E. Moya and J. Gonzalez. J. Phys. Chem. Solids **56** (1995) 481.
6) J. Gonzalez, E. Golderon, T. Tinico, J. P. Itie, A. Polian and E. Moya: J. Phys. Chem. Solids **56** (1995) 507.
7) I.I. Burlakov, Y. S. Raptis, V. V. Ursaki, E. Anastassakis and I. M. Tiginyanu: Solid State Commun. **101** (1997) 377.
8) K.-J. Range, W. Becker and A. Weiss: Z. Naturforsch. B **23** (1984) 1009.
9) S. B. Bonsall and F. A. Hummel: J. Solid State Chem. **25** (1978) 379.
10) H. Hauseler and A. Cansiz: Z. Naturforsch. B **38** (1983) 311.
11) M. E. Hills, D. C. Harris and C. K. Lowe-Ma: J. Phys. Chem. Solids **48** (1987) 501.
12) N. A. Moldovyan: Izv. Akad. Nauk SSSR, Neorg. Mater. **27** (1991) 1969.
13) I. M. Tiginyanu, P. P. Lottici, C. Razzetti and S. Gennarri. *Proc. 9th Int. Conf. Ternary and Multinary Compounds, Yokohama, 1993*, Jpn. J. Appl. Phys. **32** (1993) Suppl. 32-3, p. 561.
14) T. Kai, M. Kaifuku, I. Aksenov and K. Sato: Jpn. J. Appl. Phys. **34** (1995) 4682.
15) W.K. Unger, B. Farnworth and J. C. Irwin: Solid State Commun. **25** (1978) 913.
16) O. V. Kulikova, N. A. Moldovyan, S. M. Popov, S. I. Radautsan and A. V. Siminel: *Proc. 9th Int. Conf. Ternary and Multinary Compounds, Yokohama, 1993*, Jpn. J. Appl. Phys. **32** (1993) Suppl. 32-3, p. 586.
17) T. Irifune, K. Fujino and E. Ohtani: Nature (UK) **349** (1991) 409.
18) R. W. J. Wyckoff: *Crystal Structures* (Wiley, New York, 1963) 2nd ed., Vol. 1, p. 112.
19) K. Tsuji, Y. Katayama, N. Koyama, Y. Yamamoto, J.-Q. Chen and M. Imai: J. Non-Cryst. Solids **156-158** (1993) 540.
20) K. Tsuji, Y. Katayama, Y. Yamamoto, H. Kanda and H. Nosaka: J. Phys. Chem. Solids **56** (1995) 559.
21) Y. K. Vohra, H. Xia, A. L. Ruoff: Appl. Phys. Lett. **57** (1990) 2666.
22) J. P. Itie, A. Polian, C. Jauberthie-Carillon, E. Dartyge, A. Fontaine, H. Tolentino, G. Tourillon: Phys. Rev. B **40** (1989) 9709.
23) P. Perlin, C. Jauberthie-Carillon, J. P. Itie, A. S. Miguel, I. Grzegory, A. Polian. Phys. Rev. B **45** (1992) 83.